International Journal of Advances in Engineering and Management (IJAEM)
Volume 6, Issue 11 Nov. 2024, pp: 180-191www.ijaem.net ISSN: 2395-5252

Hydrodynamic CharacteristicsAnalysisand Simulation of water GekcoAutonomous underwater Vehicle

Keribo, Ibelema. F [(a)], Orji, Charles. U [(ab)],Tamunodukobipi, D [(b)], Douglas, Ibiba. E[(ab)]

[(a)] *Department of Marine Engineering, Faculty of Engineering, Rivers State University, Nkpolu-Oroworukwo, Port Harcourt, Nigeria*

[(b)] *NNPC/SPDC-JV Centre of Excellence in Marine and Offshore Engineering, Rivers State University, Port Harcourt, Nigeria*

Date of Submission: 01-11-2024 Date of Acceptance: 10-11-2024

ABSTRACT

The need to explore and characterize the seabed for exploitation of hydrocarbon is imperative as it plays a major role in the development of the Nigerian economy and indeed the economy of Nations. However, to achieve this in a safe, precise and cost-effective manner is a challenge that needed to be addressed. This paper presents the hydrodynamic analysis on the water gecko autonomous underwater vehicle capable of subsea subsoil characterization. The hull developed measures 3.42m long, 0.85 m wide and 0.78 m high. The mid-section of the hull Houses the cone penetration test machine, the fore section, the electronics and batteries and the rear section the hydraulic system and thruster control. Software simulation on the complex hull shape show that the total bare hull resistance is 600N at a speed of 2.4m/s. Also, the hydrodynamic coefficients of the vehicle such as the lift and drag were generated for between -15 to 30 degrees angle of attack and -15 to 15 degrees side slip angles from computational fluid dynamics (CFD) simulation. Open loop maneuverswerecarried out in the surge motion direction and simulation results show that there is a very close proximity between the designed condition and the simulated condition. In the surge motion simulation, which is the bases of the generation of the hydrodynamic coefficients it was observed that whereas a speed of 2.4m/s was used for the generation of the coefficient and a resistance of 600N was seen by the hull at that speed, a speed 2.63m/s was achieved by the vehicle when propeller by four 167N thrusters acting at 26degrees to the longitudinal axis thereby validating the inputs.

Keywords: Autonomous, Hull, Hydrodynamic, Simulation, Subsoil

I. INTRODUCTION

An autonomous underwater vehicle (AUV) is an underwater robot that can propel itself from a programmed start position and following a prescribed path without human intervention.(Jain, 2015), also known as unmanned underwater vehicle. It is driven through the water by a propulsion system, controlled and maneuverer in the three-dimensional space by an on-board computer connected to sensors and actuators that successfully accomplish prescribed tasks. Lately the use of AUVs is increased significantly as the quest to understand the depths of the ocean continues to grow. Areas of application of this type of vehicle include cable or pipeline tracking and deep ocean exploration. Different structures with different size of these AUVs are developed. Most of these AUVS are torpedo-like with streamline bodies,(Naeem, 2017)

Designing an autonomous underwater vehicle (AUV) involves a multidisciplinary approach that considers various factors, including hydrodynamics, propulsion systems, structural integrity and integration of navigation and control systems. According to Chen and Liu (2022), the propulsion system is a critical component that determines the overall performance and efficiency of an AUV. The authors discussed different propulsion systems, such as thrusters, waterjets and propellers, highlighting their respective advantages and limitations.

Several studies have explored the hydrodynamic characteristics of AUVs to

International Journal of Advances in Engineering and Management (IJAEM)
Volume 6, Issue 11 Nov. 2024, pp: 180-191www.ijaem.net ISSN: 2395-5252

optimisetheir hull forms and improve their efficiency. Nazemian and Ghadimi (2021) employed computational fluid dynamics (CFD) to optimise the hull form of a displacement trimaran, aiming to reduce its resistance in calm water and wavy conditions. Similarly, Ponzini et al., (2020) developed a web-based application for automatic CFD analysis of planing hulls, enabling easier evaluation and comparison of different hull designs. This innovative approach streamlines the design process by providing quick and accurate assessments of hydrodynamic performance, enabling designers to iterate rapidly and identify the most promising configurations. In addition to hull optimisation, the propulsion system is also crucial in determining AUV performance. Chen and Liu (2022) discussed various propulsion options, including thrusters, waterjets and propellers, each with its own set of advantages and limitations. Thrusters, as investigated by Zhang et al., (2021), offer precise control and manoeuvrability, making them well-suited for tasks requiring intricate movements or station-keeping. However, their efficiency may diminish at higher speeds or in challenging underwater environments due to increased drag and energy consumption.

The hull design of an autonomous underwater vehicle (AUV) plays a crucial role in determining its hydrodynamic performance, manoeuvrability and overall efficiency. Optimising the hull form is a complex task that involves considering various factors, including drag reduction, stability and maneuvering capabilities.

Thus, this study aims at designing an optimized AUV hull with well-defined hydrodynamic characterization for efficient motion control during seabed sampling activities. The core objective is to analyze and present the hydrodynamic features of the design for efficient motion control.

II. MATERIALS

Determination of Hydrostatic and Hydrodynamic parameters

The hydrostatic and hydrodynamic parameters necessary for the simulation of the AUV motion were obtained using MAXSURF.

MAXSURF Naval Architecture Software

MAXSURF is an integrated naval architectural tool that can be used to determine the resistance, stability, structural integrity etc of marine vehicles. The resistance of the AUV was obtained using Maxsurf Naval Architecture software and the result is presented in the Figure 12.

AutodeskInventor

The other software used in this work is the Autodesk Inventor which is used to create a 3D parametric model of the AUV and to determine the structural integrity of the vehicle. Autodesk inventor is a parametric 3D modelling software with the capability of carrying out stress analysis on structures and vessels that are subjected to pressure loads. The components of the design process obtained from the software are:

1. 3D model of the vehicle shown in Figure 1.
2. Structural arrangement of the complex internal system architecture
3. Stress analysis of the AUV hull
4. Centre of gravity of the system
5. Inertia mass matrix

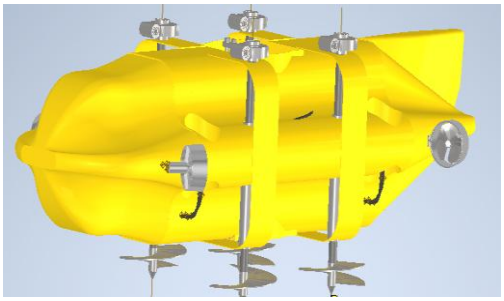

Figure 1:Model of AUV in ANSYS

The Figure 2 shows the AUV model imported into ANSYS spaceclaim. The geometry is cleaned and made watertight, and enclosure added with a body of influence included to refine the mesh size around the model.

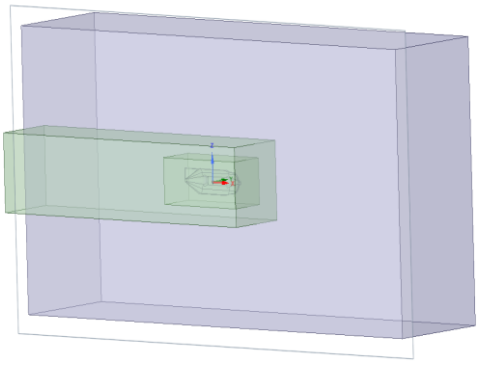

Figure 2: AUV model imported into ANSYS spaceclaim

The Figure 3 (a) and (b) show the model meshed with the surrounding environment (enclosure) and the body of influence. The

International Journal of Advances in Engineering and Management (IJAEM)
Volume 6, Issue 11 Nov. 2024, pp: 180-191www.ijaem.net ISSN: 2395-5252

enclosure mesh size is coarserwhile a finer mesh size was used within the boundaries of the body of influence.

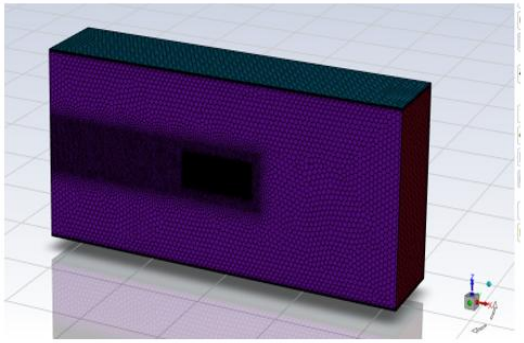

(a) Mesh Characteristics in the ANSYS Spaceclaim

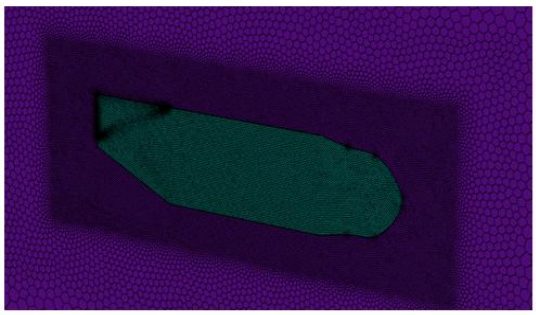

(b) AUV Discretized Body

Figure 3: Meshed AUV models

The Figure 4 shows the reference inputs used in the simulation of the model obtained from the geometric size, material and physical properties of the model and the interacting fluid medium. The velocity of the fluid is the same as the velocity of the AUV at which the resistance of the AUV has been determined using MAXSURF. The simulation was post processed to determine the hydrodynamic coefficients in all six degrees of freedom. This was carried out for a combination of angle of attack between -15 and 30 degrees and side slip angle of -15- and 15-degrees results are presented in the next section

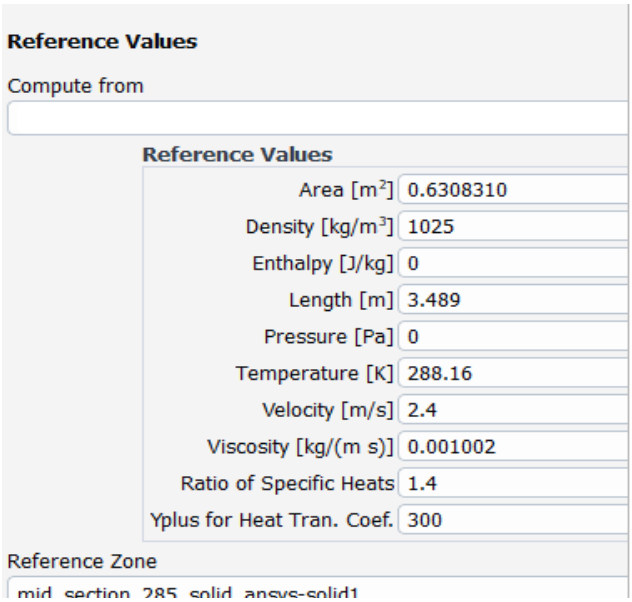

Figure 4: shows the Reference Inputs in the Solution

International Journal of Advances in Engineering and Management (IJAEM)
Volume 6, Issue 11 Nov. 2024, pp: 180-191www.ijaem.net ISSN: 2395-5252

III. METHODS

Implementation of Hydrodynamic Coefficients in MATLAB

Figure 5 shows the Simulink model of the implementation of the hydrodynamic coefficients in MATLAB.The angular orientation of the vehicle alpha is read and the hydrodynamic coefficient for that angle is looked up and applied to the equation of motion to determine the characteristic fluid hull interaction.

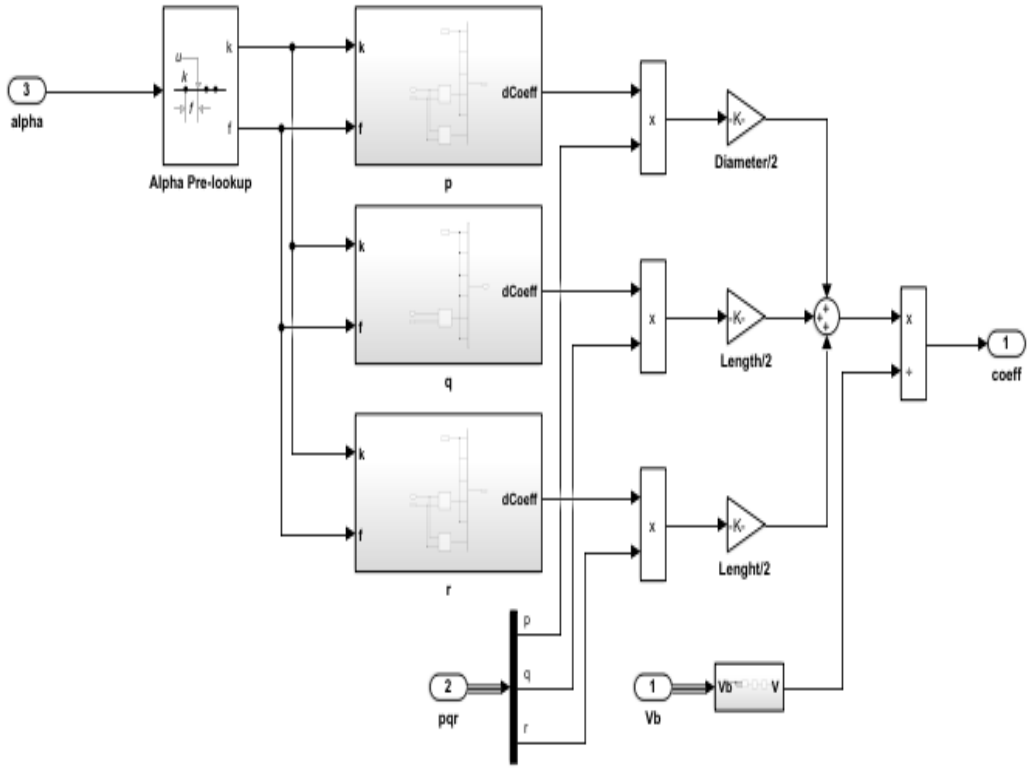

Figure 5: Hydrodynamic Coefficients Combination for Different Orientations in Simulink

IV. RESULTS AND DISCUSSIONS

Lift and Drag (hydrodynamic Coefficients)

Figures6 to 11 showthe plot of the hydrodynamic coefficients of the AUV obtained from ANSYS Fluent analysis as a combination of angle of attack and side slip angle while Figures 12 to 17 shows the hydrodynamic damping coefficients.

Hydrodynamic Coefficient CX

This CX is the drag coefficient of the AUV body as generated from the ANSYS analysis.The plot in Figure 6 shows that the drag coefficient increases with increase in inside slip angle and the angle of attack. The maximum drag is almost 3 at a side slip angle of -15- and -15-degrees angle of attack to a minimum of almost about 0.15 at 0 degrees and then increases again in the same manner as the angle increases.

International Journal of Advances in Engineering and Management (IJAEM)
Volume 6, Issue 11 Nov. 2024, pp: 180-191www.ijaem.net ISSN: 2395-5252

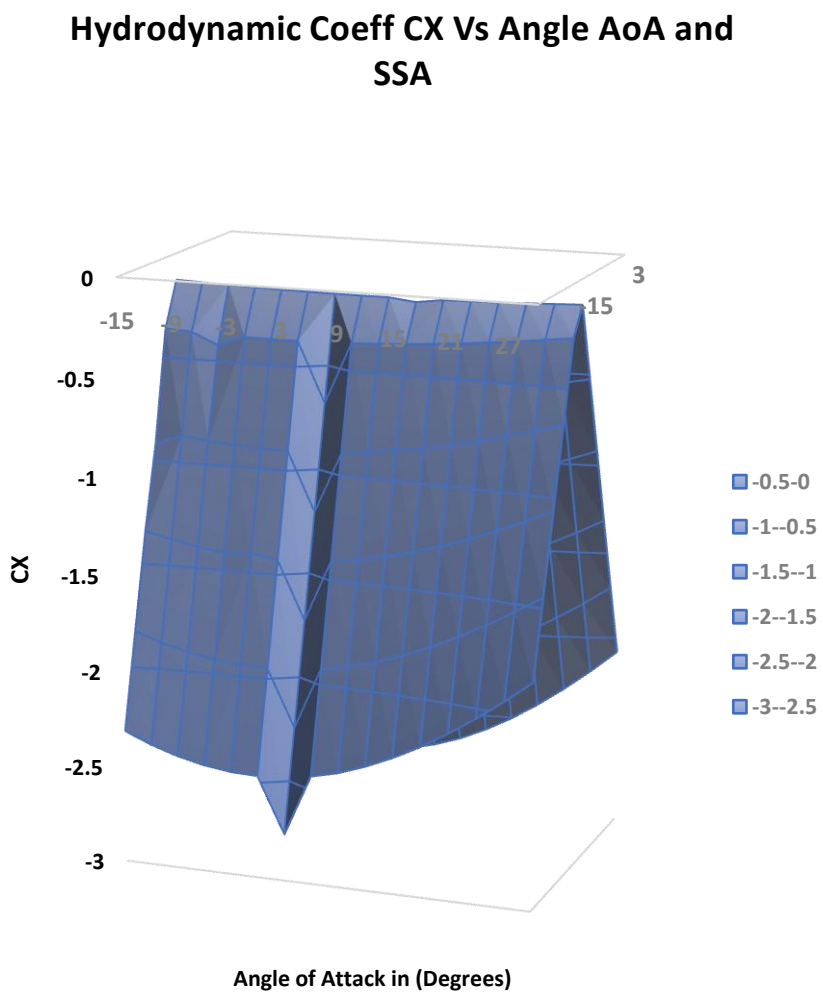

Figure 6: Hydrodynamic Coefficient (CX) at Varying AoA and SSA

Lateral Force Coefficient

Figure 7 shows the hydrodynamic coefficient CY, the lateral force coefficient that describes the hydrodynamic resistance of the AUV in the lateral direction. The force as can be observed from the plot decreases with an increase in the side slip angle to a minimum at 0 degrees from -15 and then increases with increasing angle of attack. The force also decreases very minimally with increase in the angle of attack. The trend described above is in line with expectation as the projected area varies accordingly.

International Journal of Advances in Engineering and Management (IJAEM)
Volume 6, Issue 11 Nov. 2024, pp: 180-191www.ijaem.net ISSN: 2395-5252

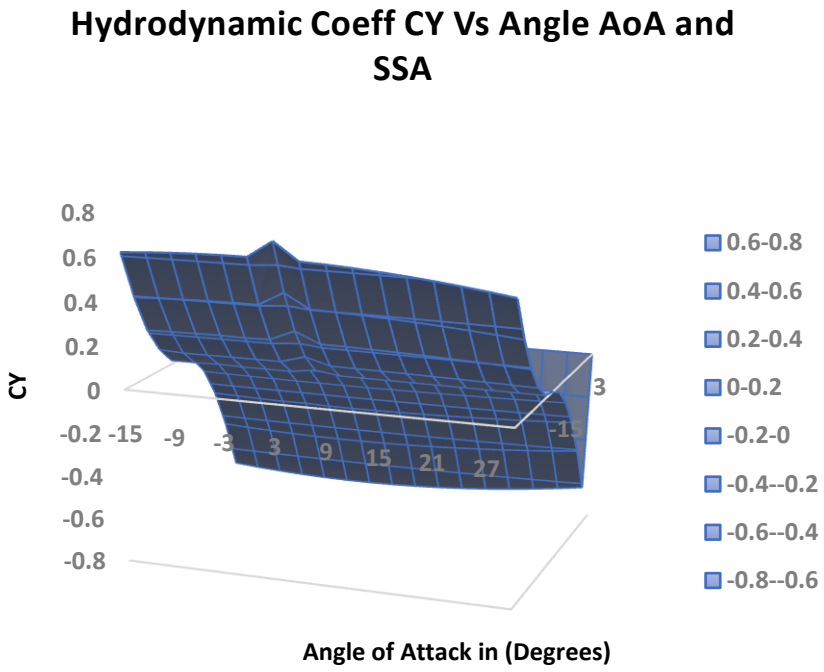

Figure 7: Hydrodynamic Coefficient (CY) at Varying AoA and SSA

Lift Coefficient of the AUV (CZ)

Figure 8 shows the hydrodynamic coefficient CZ, the lift coefficient which is a dimensionless number that describes the hydrodynamic force on the AUV in the vertical direction. The force as can be observed from the plot decreases with an increase in the side slip angle to a minimum at 0 degrees from -15 and then increases with increasing angle of attack from -15 degrees to 0 degrees. Also, from 0 degrees to 30 degrees, the coefficient increases with both increase in inside slip angle and angle of attack to 0 degrees from -15 degrees and decreases from 0 to 15 degrees.

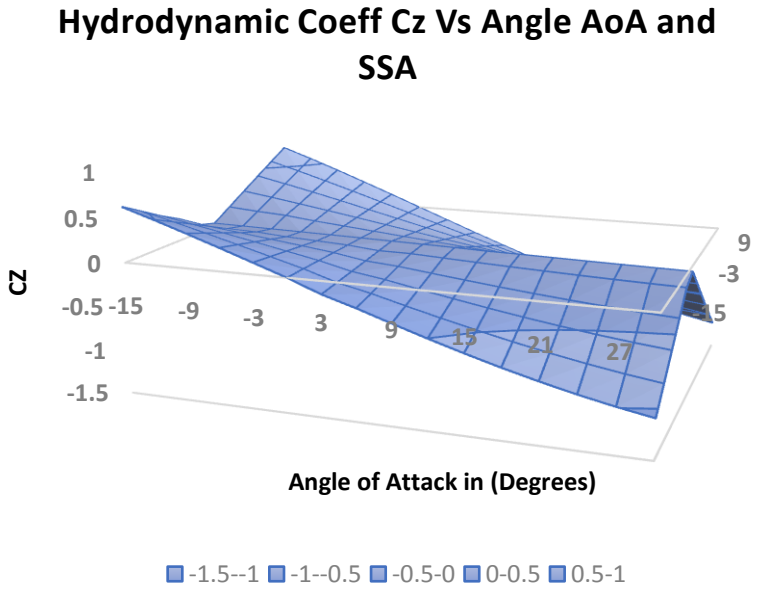

Figure 8: Hydrodynamic Coefficient (CZ) at Varying AoA and SSA

International Journal of Advances in Engineering and Management (IJAEM)
Volume 6, Issue 11 Nov. 2024, pp: 180-191www.ijaem.net ISSN: 2395-5252

Hydrodynamic Roll Moment Coefficient (CMK)

Figure 9 show a plot of the Roll moment coefficient, which is a measure of the rotational forces acting on the AUV about the x axis in a fluid. The moments are plotted against varying angle of attack and the side slip angle. Generally, it can be observed from the plot that as the AoA increases, CMK shows minimal linear decrease while the moment coefficient is unaffected by the increase in the side slip angle, indicating a decrease in the rotational forces at higher angles of attack up to -12 degrees. Then the trend changes to an increase in the moment coefficient with an increase in the angle of attack up to 30 degrees. This trend continues from after 0 degrees side slip angle to 15 degrees but in the opposite sense as outlined above.

The effect of high CMK is rotational instability of the vehicle. Here in this work, we have seen the roll moment coefficient to be decreasing with increasing angle of attack which indicates good stability characteristics and Control.

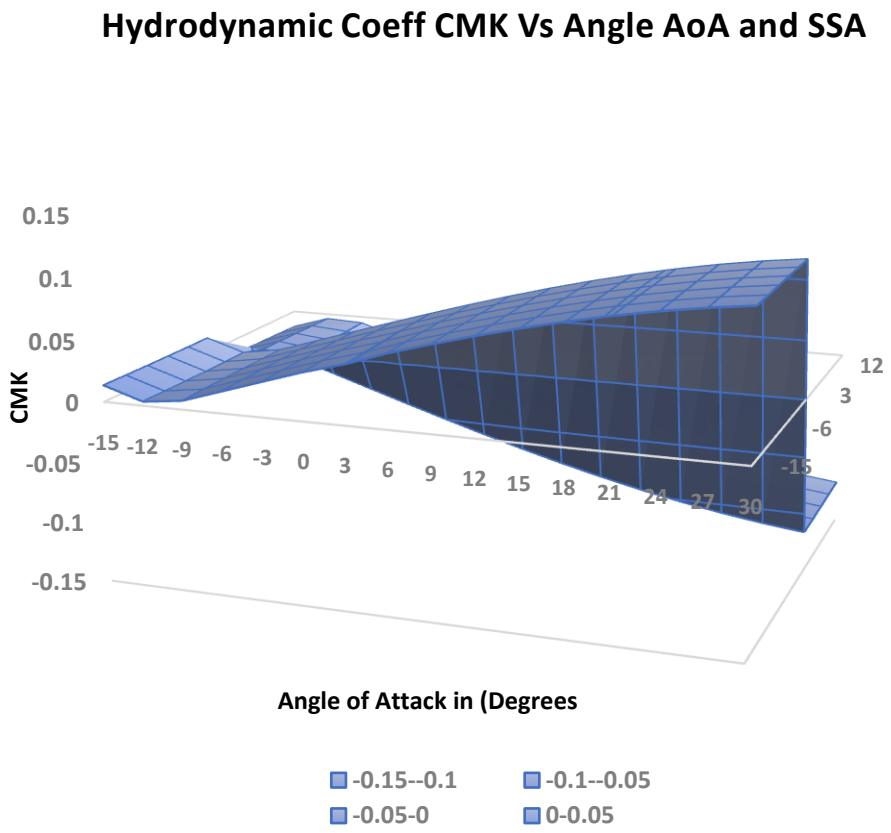

Figure 9: Hydrodynamic Coefficient (CMK) at Varying AoA and SSA

Hydrodynamic Pitch Moment Coefficient (CMM)

Figure 10 show a plot of the Pitch moment coefficient, which is a measure of the rotational forces acting on the AUV about the y axis in a fluid. The moments are plotted against varying angle of attack and the side slip angle. Generally, it can be observed from the plot that as the AoA and the side slip angle increases, CMK shows minimal linear decrease of the moment coefficient, indicating a decrease in the rotational forces at higher angles of attack up to -12 degrees angle of attack and 0 degrees side slip angel. Then the trend changes to a minimal increase in the moment coefficient with an increase in the angle of attack and a decrease in the moment with increases in the side slip angle up to -3 degrees and zero degrees respectively.

The effect of high CMM is rotational instability of the vehicle. Here in this work, we have seen the roll moment coefficient to be decreasing with increasing angle of attack which indicates good stability characteristics and Control.

International Journal of Advances in Engineering and Management (IJAEM)
Volume 6, Issue 11 Nov. 2024, pp: 180-191www.ijaem.net ISSN: 2395-5252

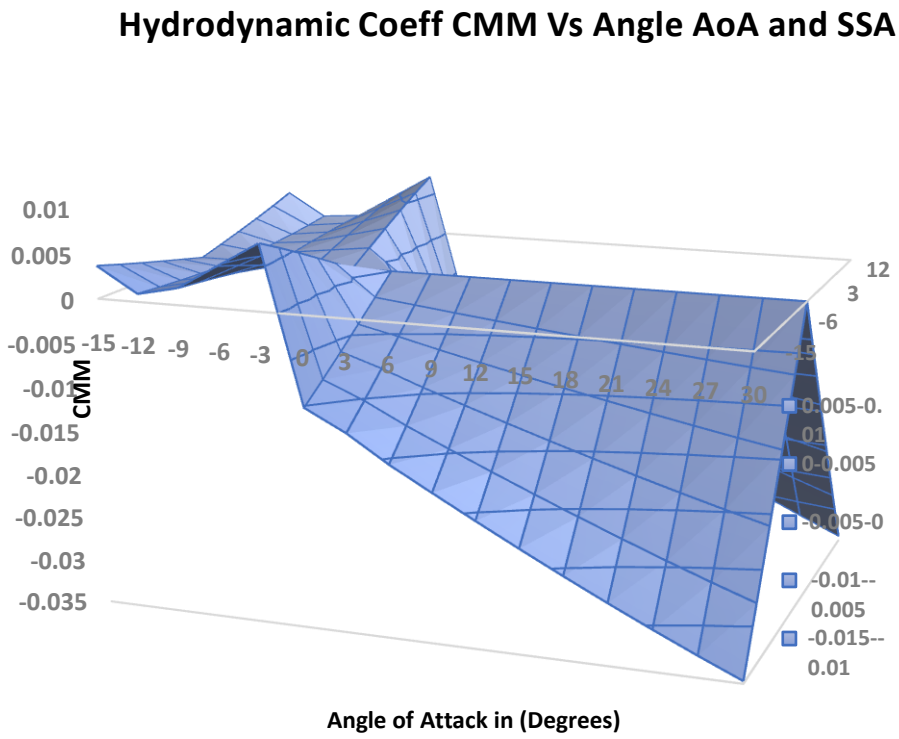

Figure 10: Hydrodynamic Coefficient (CMM) at Varying AoA and SSA

Yaw Moment Coefficient (CMN)

Figure 11 show a plot of the yaw moment coefficient, which is a measure of the rotational forces acting on the AUV about the z axis in a fluid. The moments are plotted against varying angles of attack and the side slip angles. Generally, it can be observed from the plot that as the AoA increases, CMN shows a non-linear decrease while the moment coefficient is unaffected by the increase in the side slip angle, indicating reduction in rotational forces at higher angles of attack. This trend is seen to continue from -15 degrees to 30 degrees angle of attack, and from -15 degrees to 0-degree side slip angle.

The effect of high CMN is instability of the vehicle. Here in this work, we have seen the yaw moment coefficient to be decreasing with increasing angle of attack which indicates good stability characteristics and Control.

International Journal of Advances in Engineering and Management (IJAEM)
Volume 6, Issue 11 Nov. 2024, pp: 180-191www.ijaem.net ISSN: 2395-5252

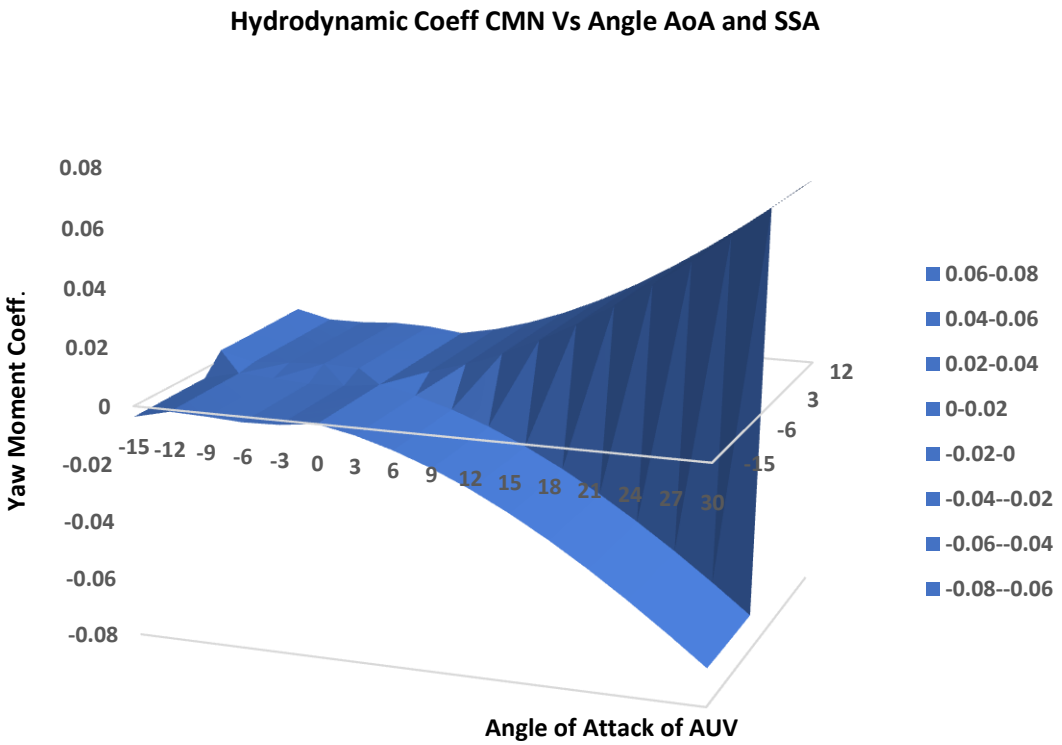

Figure 11: Hydrodynamic Coefficient (CMN) at Varying AoA and SSA

Resistance of AUV

Figure 12 shows the result of the hydrodynamic resistance analysis.Based on the AUV requirements for maximum operating speed at 2.4 m/s, a resistance of 600N was observed. Other data obtained are the added mass coefficients and the damping coefficients.

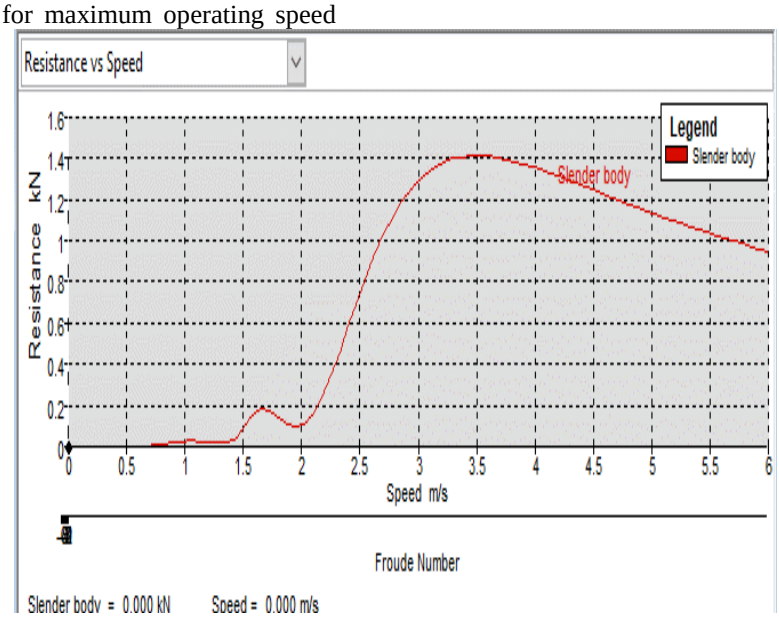

Figure 12: Resistance Versus Speed

International Journal of Advances in Engineering and Management (IJAEM)
Volume 6, Issue 11 Nov. 2024, pp: 180-191www.ijaem.net ISSN: 2395-5252

Open Loop Surge Simulation

The surge simulation is performed using SIMSCAPE multibody connected with Simulink and being driven on the MATLAB platform. Figures13 and 14 show the AUV's Elevation and plan views respectively while flying under water, Here the hydrodynamic coefficients obtained earlier are applied, a thrust of 167N which translates to a horizontal thrust of 150 N for each of the horizontal thruster, cumulating to a total of 600 N for the surge motion is implemented. The Figure 15 shows the plot from the surge maneuver wherethe acceleration, position and velocity plots are shown and labelled as a, p, and v respectively. From the plots it can be observed that an increasing acceleration in one minute gave rise to a maximum velocity of 2.62m/s at about 52seconds and then plateaued and started decelerating. This trend is very close to expectation given that the design speed based on which the hydrodynamic coefficient for the surge motion is generated is 2.4m/s. Also, this validates the propulsion force simulated from MAXSURF where a velocity of 2.4m/s generated a resistance of 600N.

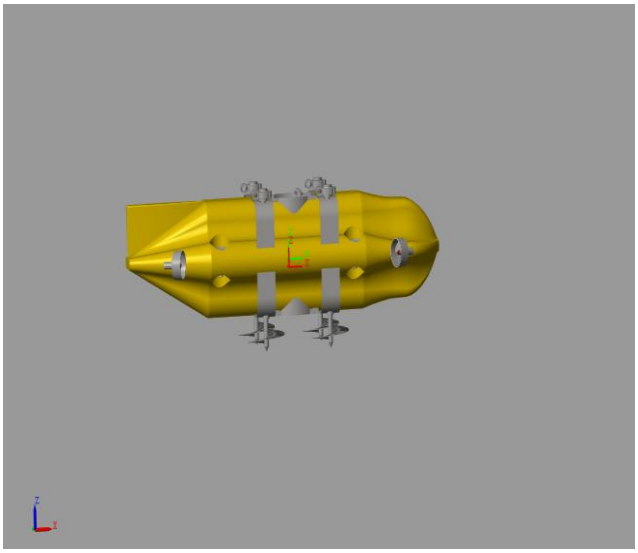

Figure 13:Elevation View of AUV Flying Under Water

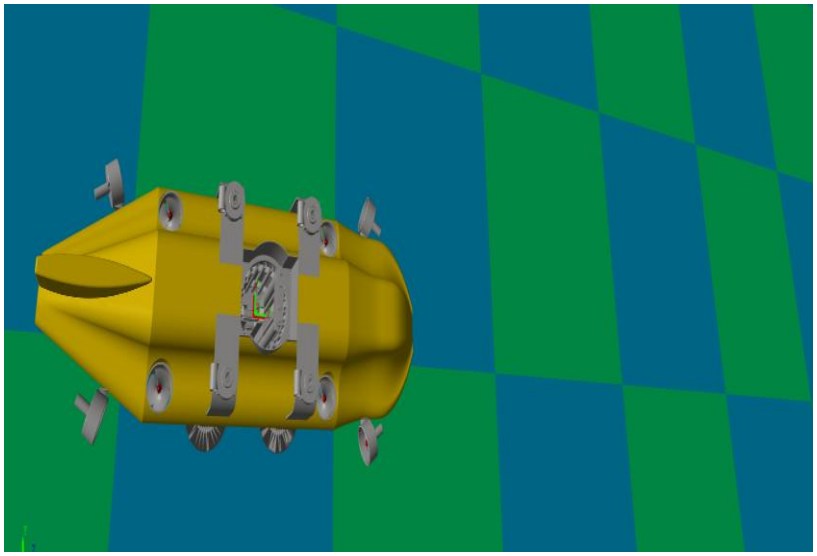

Figure 14: Top View of AUV Flying Under Water

International Journal of Advances in Engineering and Management (IJAEM)
Volume 6, Issue 11 Nov. 2024, pp: 180-191www.ijaem.net ISSN: 2395-5252

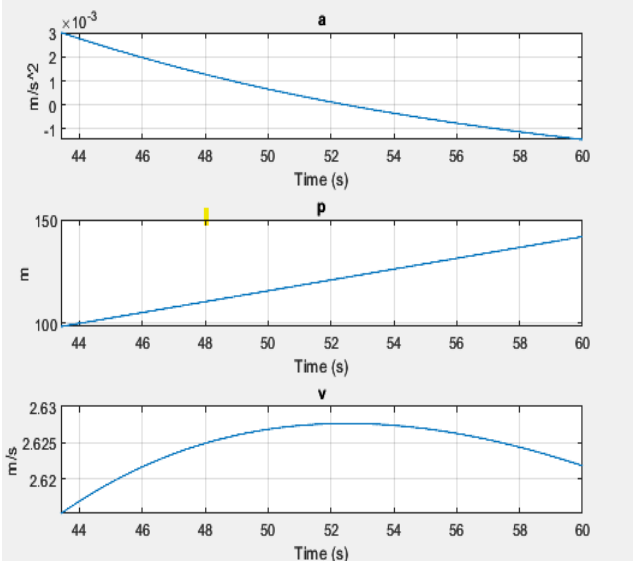

Figure 15: Plot of Acceleration Displacement andVelocity of AUV

V. CONCLUSION

The hydrostatic and restance parameters for the hull were simulated using MAXSURF. Here a three percent buoyancy was initiated in order that the analysis could be carried out. The hydrodynamic coefficients were obtained from ANSYS simulation and post processing calculations. The coefficients were obtained at various angles of attack (-15 to30 degrees) and side slip angles (15 to 15 degrees). This is done to develop a three dimensional look up table that when implemented in the vehicle simulation in MATLAB, will give a good fidelity model. The simulation of the vehicle motion in MATLAB is carried out by implementing the six degree of freedom equation. The simulation results show that there is a very close proximity between the designed condition and the simulated condition. In the surge motion simulation, which is the bases of the generation of the hydrodynamic coefficients it was observed that whereas a speed of 2.4m/s was used as the for the generation of the coefficient and a resistance of 600N was seen by the hull at that speed, a speed 2.63m/s was achieved by the vehicle thereby validating the inputs

Nomenclature

AUV -Autonomous Underwater Vehicle

CFD - Computational Fluid Dynamics

TAN - Terrain Aided Navigation

DVL - Doppler Velocity Logger

USBL - Ultrashort Base Line

LBL - Long Base Line

MPC - Model Predictive Control

COTS - Commercial Off the Shelf

MR - Mixed Reality

ROV - Remotely Operated Vehicle

CPT - Cone Penetration Test Machine

AI - Artificial Intelligence

REFERENCES

[1]. Experiments. Journal of Marine Science and Engineering, 11(9). https://doi.org/10.3390/jmse11091744

[2]. Ge, Z., Luo, Q., Jin, C., & Liang, G. (2016). Modeling and diving control of a vector propulsion AUV. 2016 IEEE International Conference on Robotics and Biomimetics, ROBIO 2016. https://doi.org/10.1109/ROBIO.2016.7866266

[3]. González-García, J., Gómez-Espinosa, A., Cuan-Urquizo, E., García-Valdovinos, L. G., Salgado-Jiménez, T., & Escobedo

Cabello, J. A. (2020). Autonomous underwater vehicles: Localization, navigation, and communication for collaborative missions. In Applied Sciences (Switzerland) (Vol. 10, Issue 4). https://doi.org/10.3390/app10041256

[4]. Grigoropoulos, G. J., Bakirtzoglou, C., Papadakis, G., &Ntouras, D. (2021). Mixed-fidelity design optimization of hull form using cfd and potential flow solvers. Journal of Marine Science and Engineering, 9(11). https://doi.org/10.3390/jmse9111234

[5]. Guo, J., Li, D., & He, B. (2021). Intelligent Collaborative Navigation and Control for AUV Tracking. IEEE Transactions on Industrial Informatics, 17(3). https://doi.org/10.1109/TII.2020.2994586

[6]. Guo, J., Zhang, Y., Chen, Z., & Feng, Y. (2020). CFD-based multi-objective optimization of a waterjet-propelled trimaran. Ocean Engineering, 195. https://doi.org/10.1016/j.oceaneng.2019.106755

[7]. Hasan, K., Ahmad, S., Liaf, A. F., Karimi, M., Ahmed, T., Shawon, M. A., &Mekhilef, S. (2024). Oceanic Challenges to Technological Solutions: A Review of Autonomous Underwater Vehicle Path Technologies in Biomimicry, Control, Navigation and Sensing. IEEE Access. https://doi.org/10.1109/ACCESS.2024.3380458

[8]. He, Y., Wang, D. B., & Ali, Z. A. (2020). A review of different designs and control models of remotely operated underwater vehicle. Measurement and Control (United Kingdom), 53(9–10). https://doi.org/10.1177/0020294020952483

[9]. Herlambang, T., Nurhadi, H., &Subchan. (2014). Preliminary numerical study on designing navigation and stability control systems for ITS AUV. Applied Mechanics and Materials, 493. https://doi.org/10.4028/www.scientific.net/AMM.493.420

[10]. He, B., Zhang, H., Li, C., Zhang, S., Liang, Y., & Yan, T. (2011). Autonomous Navigation for Autonomous Underwater Vehicles. Sensors, 110959-10980.